Submitted on 19 Jul 2026

Referee #2: Xiangrui Kong, kongx@chem.gu.se

Suggestions for revision or reasons for rejection

The authors have substantively addressed the concerns and questions.

I recommend acceptance subject to minor revisions:

1. The discussion of OH suppression/RO2 alteration remains qualitative. A quantitative estimate for the OH exposure range used would strengthen it, or state explicitly that this cannot be quantified.

2. Minor grammatical issues remain in revised text: Section 3.4: "is in consistent with," "somehow reasonable".

These are technical items; no further external review is needed.

Response: Thank you for this positive assessment and for identifying the remaining technical issues. For point 1 you have mentioned, OH suppression and RO_2 alternation mention in Section 2.1 are possible artifacts on oxidation reactions that may possibly happen during OH oxidation reactions in Go:PAM reactors and lead to possible bias between oxidation chemistry in the reactor and real atmosphere. The experiment did not directly measure OH suppression, altered RO_2 chemistry, secondary photolysis, or fragmentation. We therefore cannot quantitatively constrain their magnitudes over the investigated OH-exposure range. This study mainly focuses on composition characteristic of gas-phase and aerosol phase cooking emissions, discussions about radical chemistry mechanisms aims at clarifying possible uncertainties and their causes, serving a possible starting point for further research. We would further clarify this point in the main text. For point 2 you have mentions, the minor grammar mistakes have been checked and modifies again. The corresponding text in Section 2.1 are shown below:

It should be noted that, the use of an OFR utilization in oxidation simulation experiments can introduce OH suppression, altered RO2 chemistry, causing secondary photolysis, and resulting in enhanced fragmentation; thus, the chemical environment of oxidation in Go:PAM might differ from that of real atmosphere, therefore, e.g. the OH-exposure-to-atmospheric-age conversion is used only as an approximate reference(Peng and Jimenez, 2020).

Submitted on 31 Jul 2026

Anonymous referee #1

Suggestions for revision or reasons for rejection

Shen et al. have addressed most of my previous comments, and the revised manuscript has improved substantially. I am satisfied with many of the revisions, particularly the expanded partitioning analysis. However, several issues concerning interpretation, presentation, and PMF robustness should still be addressed before publication in ACP.

1. Section 3.1 and Figure 1: nucleation, condensation, and coagulation

The discussion should distinguish particle formation from particle growth. The appearance of

a sub-50 nm mode and the increase in particle number are consistent with continued new particle formation by nucleation, whereas the increase in modal diameter from 14.1 to 31.1 nm and the increase in aerosol mass indicate subsequent condensational growth. The increase in number concentration suggests that coagulation is unlikely to dominate, since coagulation alone would reduce particle number, although its contribution cannot be completely excluded.

I therefore suggest describing the process as nucleation followed by predominantly condensational growth. The fact that the secondary mode is smaller than the primary mode does not contradict condensation because these are different particle populations. If the authors wish to conclude that mass growth is controlled primarily by increasing particle size rather than number, this should be supported using integrated volume or mass distributions rather than modal diameter alone. Similarly, the timescale comparison at Lines 343-344 does not by itself demonstrate that condensation dominates over coagulation and should be qualified.

Response: Thank you for your advice. For discussion in section 3.1, we have defined particles detected with diameter lower than 20nm as nuclear mode, 20-100nm as Aitken mode, and >100nm as accumulation mode. Nuclear mode particles stand for particles generated from particle formation, Aitken mode particles are from particle condensational growth, accumulation mode are mostly primary particles. We calculate mass and number concentration of nucleation mode particles so as to clarify the contribution of nucleation to SOA formation. We have found out that the number concentration of nuclear mode particles exhibits a decreasing trend with enhancement of OH exposure and SOA number/mass concentration growth(from 9.61 to 7.66×10^{5} #·cm^{-3}), and mass concentration is kept within range of 1.75~2 μg·m^{-3}. These results indicate major contribution of gas-phase compounds condensing onto existing particle in SOA growth, while formation of nucleation mode particles serve as an initialization process in SOA formation and growth. Modified section 3.1 is shown here:

Figure 1 illustrates evolution of size and mass distributions from primary to secondary cooking aerosols with enhancement of OH exposure throughout oxidation experiment. Detailed size and mass distribution characteristics of aerosols are shown in **Table S6.1**, **Supplement S1.** Primary cooking aerosols exhibit a relatively broad size distribution, with particle diameters ranging from 50 to 300 nm. These particles are generally formed through physical processes such as oil evaporation, or thermal chemical reactions including oxidation and decomposition. Primary cooking aerosols comprise of components with large molecular size and relatively low carbon oxidation states, such as long-chain alkanes, alkenes, alkanals, alkenones, fatty acids and their glycerol esters, and steroids(Rogge et al., 1991; Nolte et al., 1999). In contrast, secondary organic aerosols are predominantly nanoparticles exhibiting monomodal distribution, with major aerosols diameter below 50 nm. SOA mass and size distribution exhibits rapid and substantial increase in both number and mass once exposed to OH radical as oxidant, even under the lowest OH concentration conditions, secondary aerosol number concentrations can reach up to 10^{6} #·cm^{-3}. Mode diameter of SOA increased from 14.1nm to 31.1nm with enhancement of OH exposure from ~10^{9} to 10^{10} #·cm^{-3}·s,

accounting for particle mass growth factor of $(31.1/14.1)^3$~10, while total number concentration increases from 1.37 to 3.42×10^6 #·cm^{-3}, accounting for particle mass growth factor of ~2.5. Moreover, as OH exposure growth, the number concentration of nuclear mode (d_p<20nm) decreases from 9.61 to 7.66×10^5 #·cm^{-3}, mass concentration is kept around 1.75~2 μg·m^{-3}. Evolution of Size and mass distribution with enhancement of OH exposure indicate that increasing OH exposure further enhances mass concentration predominately through particle size growth rather than number increase, implying that the dominate driving force of SOA growth is condensation of gas-phase products, while formation of new particles serve as initialization process of SOA formation and growth. For particles larger than 90 nm where primary aerosols are most abundant in, enhancement of OH exposure result in minimal changes in number and mass concentration, with average declination of less than 20% even under the highest OH exposure conditions (**Fig. S6.1**, **Supplement S1**). These findings collectively suggest that secondary organic aerosols from oil boiling originate mainly from condensation of gas-phase oxidation products to form nucleation and Aitken mode particles, rather than oxidative aging and modification of primary aerosols in accumulation mode(Tan et al., 2023; Zhang et al., 2023). The observed low reactivity of primary cooking aerosols during oxidation may be attributed to the low miscibility between nonpolar or low-polarity primary components and newly formed highly polar secondary compounds likely resulting from limited partitioning tendency of primary components, or lower number concentration and specific surface area of primary aerosols from oil-boiling activities than secondary cooking aerosols even at the lowest OH exposure, leading to limited gas-particle partitioning rate(Chandramouli et al., 2003; Milsom et al., 2021; Liu et al., 2025).

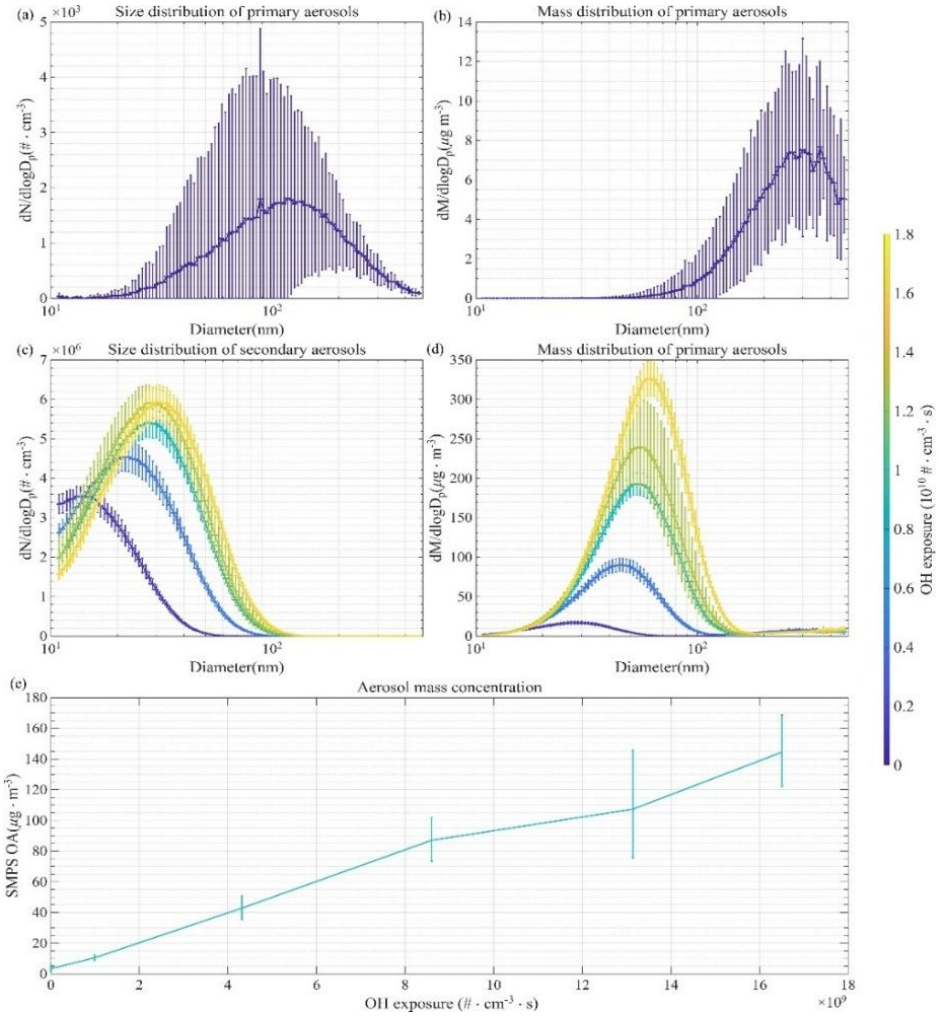

Figure 1 in main text. Primary and Secondary aerosol size & mass distribution evolution with OH exposure increases. (a) (b)illustrate size and mass distribution of primary particles, (c) (d) size and mass distribution of secondary aerosols at OH exposure 0.1~1.8×10^{10} cm^{-3} s. (e) exhibits mass concentration evolution with oxidation process from primary to OH exposure 1.8×10^{10} cm^{-3} s.

2. Lines 193-204 and Figure 2: compositional evolution and mechanistic interpretation

The authors report increasing gas-phase molecular size with nearly constant (OS_C), while particle-phase molecular size and (OS_C) change only slightly. These trends are then used to conclude that SOA formation is governed primarily by gas-phase oxidation followed by condensation rather than particle-phase oxidation. However, the trends are difficult to evaluate from Figure 2. Table 1 also shows that the interpretation depends on whether the primary condition is included: both phases exhibit appreciable changes from the primary to the first oxidized condition but remain relatively stable among the oxidized conditions. Please clarify the comparison being made and present molecular size and (OS_C) versus OH exposure separately for each phase.

More importantly, differences in bulk (OS_C) alone do not establish the dominant oxidation pathway. They may also reflect changing composition, gas-particle partitioning, detection sensitivity, or thermal-decomposition artifacts. Unless additional phase-resolved evidence is

provided, the authors should describe the observations as being consistent with, rather than demonstrating, gas-phase oxidation followed by condensation.

Response: Thank you for your advice. Figure 2 shows 2-D-VBS distribution evolution of primary and secondary aerosols, which may be somewhat complex to recognize the bulk volatility and oxidative state changes. The distribution of volatility does shows increasing amount of S/IVOCs (especially SVOC) and some LVOCs at average OS_C ~-0.75 Detailed bulk composition evolutions are shown in Table 1. Briefly, with oxidation proceeds and OH exposure enhance to maximum, the mean composition changes from $C_{3.5}H_{5.4}O_{2.6}N_{0.03}S_{0.01}$ to $C_{7.0}H_{11.0}O_{4.2}N_{0.07}S_{0.06}$ in gas phase and from $C_{7.1}H_{10.3}O_{3.8}N_{0.09}S_{0.03}$ to $C_{7.8}H_{13.0}O_{4.1}N_{0.04}S_{0.01}$ in aerosol phase. The mean C^0(in $\mu g \cdot m^{-3}$) change from $10^{6.0}$ to $10^{2.3}$ in gas phase, from $10^{2.8}$ to $10^{2.2}$ in aerosol phase. The mean OS_C keep around -0.45 in gas phase and -0.65 in aerosol phase. Most abundant species in primary emissions are IVOCs and VOCs, while abundance of SVOC and LVOC growth significantly with OH exposure enhancement. On the other hand, OS_c variations with OH exposure enhancements are relatively minor, which may uncover that SOA formation and growth is based on continuous condensation of secondary products in aerosol phase rather than continuous oxidation of gas-phase and aerosol-phase oxidation products. The unexpected higher OS_C of primary aerosols especially in gas phase are due to glycerol related compounds, while SOA are generated from oxidation of fatty-acid chains. Changes in Text of section 3.2 are shown below. For SOA formation mechanism hypothesis based on composition evolution, the uncertainties are shown in text, and a more cautious clarity and conclusion are adopted. Modified section 3.2 is shown here:

Figure 2 displays the volatility and compositional distribution of cooking aerosols and associated gas-phase organic components within the two-dimensional volatility basis set (2-D VBS) framework (Donahue et al., 2012). Average composition and volatility evolution are shown in **Table 1**. The majority of primary and secondary organic species are distributed in the semi-volatile and intermediate-volatile organic compound (S/IVOC) range, with an average carbon oxidation state (OSc) spanning from –1.25 to 0.5. Throughout the oxidation experiment, increasing OH exposure led to a substantial enhancement of S/IVOC components, consistent with the trend observed for aerosol particles. Additionally, the formation of low-volatility, highly oxidized compounds (classified as LVOC) derived possibly from multi-generation oxidation is also promoted.

In gas phase, the average molecular size increases significantly during oxidation, whereas the carbon oxidation state remains nearly constant or exhibits a slight decrease following OH radical addition. This behavior may be attributed to the generation of gas-phase oxidation products via cleavage of primary long-chain fatty acids, polymerization among oxidation intermediates such as RO_2 and RO radicals, and the oxidative depletion of primary low-molecular-weight organic acids resulting from glycerol thermal decomposition, such as formic acid, acetic acid, and glyceric acid (Zhang et al., 2018; Takhar et al., 2022). By contrast, compositional shifts in the aerosol phase within the 2-D VBS space—such as in oxidation state and molecular size—are relatively minor compared to those in the gas phase. The oxidative state changes of particle-phase organics with enhanced OH exposure is relatively minor, with only marginal growth in molecular dimensions. The relatively small molecular size of primary cooking aerosols may result from the limited detection sensitivity of iodide-adduct CIMS toward nonpolar or low-polarity compounds with large molecular weights

and fewer oxygen-containing functional groups, e.g., long-chain hydrocarbons, fatty acids, and steroids (Iyer et al., 2016). These compositional patterns suggest that gas-phase oxidative formation and condensation of secondary gas phase S/IVOCs onto SOA particles would serve as a more predominately source of SOA formation and growth, rather than by continuous oxidation within the particle phase. Observation implies that the oxidation process in the flow tube would have been approaching a "steady-state turning point" with enhancement of OH exposure because of the formation of higher-oxidized and lower-volatile oxidation products. These products, formed through oxidation of long-chain primary acids and carbonyls, exhibit lower volatility, higher viscosity and lower oxidation rate, thereby slowing subsequent oxidative aging (Milsom et al., 2021). Particle-phase products reach this stage earlier owing to their oxygen-rich nature, such as major abundance of $C_{>6}$ dicarboxylic acids and peroxides. The somehow close average volatility between gas-phase and aerosol phase would possibly show underlying kinetic and thermodynamic mechanisms. Note that measurement and estimation uncertainty of FIGAERO-CIMS and 2-D-VBS, including thermal decomposition, might influence the results. Detailed 2-D VBS distribution of primary and secondary organic matter in gas and aerosol phase are shown in **Supplementary Material S2**.

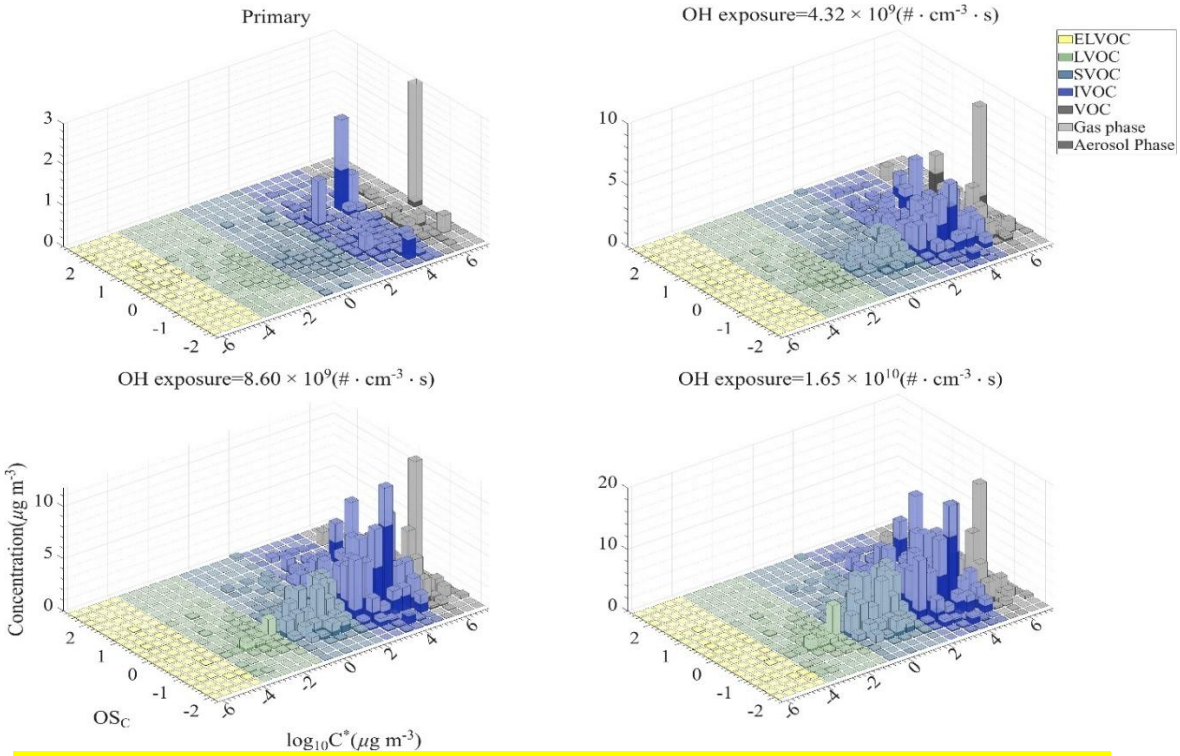

Figure 2 In Main Text Distribution of gas-phase and aerosol-phase primary and secondary cooking organic species in 2-D VBS space with oxidation

3. Lines 203-204: FIGAERO thermal-decomposition artifacts

The interpretation of particle-phase molecular composition may be affected by thermal decomposition of dimers, oligomers, peroxides, or other thermally labile compounds during FIGAERO desorption. This is particularly relevant because the manuscript identifies a PMF factor associated with thermal decomposition.

Please explain how suspected decomposition products were identified and treated in Figure 2 and Table 1. Thermograms may indicate thermal decomposition, but they cannot necessarily establish that a detected formula represents an intact monomer. The resulting uncertainty should therefore be acknowledged.

Response: Thank you for your advice. Thermal-decomposition is one of the typical system measurement uncertainties in FIGAERO-CIMS instrumentations. We have mentioned the uncertainty in section 3.2, and utilize peak temperature methods in thermodynamic analysis section as reference thermodynamic property estimation methods to account for thermal desorption influence. Briefly, if a compound or a PMF factor have a significant higher formula-based volatility than gas-particle-partitioning-based or thermogram-based volatility, the compounds would be treated as possible thermal-decomposition-related compound or factor, e.g. factor LV-OxiGen^{1st}-Gly^{TD}. The influence of thermal desorption has been discussed in section 3.3, shown below:

Factor LV-OxiGen^{1st}-Gly^{TD} have similar average oxidative state and molecular size with V-OxiGen^{1st}-Gly, seems corresponding to gas phase portion of first-generation oxidation products represented by V-OxiGen^{1st}-Gly. However, thermal desorption thermogram of LV-OxiGen^{1st}-Gly^{TD} peaks at ~440K, showing that compounds represented by LV-OxiGen^{1st}-Gly^{TD} have much lower volatility than molecular composition corresponding to this factor, indicating that LV-OxiGen^{1st}-Gly^{TD} representing thermal decomposition fragmentations of oxidation products with long-chain fatty acid structure (Frankel et al., 1983; Patrikios et al., 1994; Martins et al., 2013; Aladedunye, 2016; Bonetti and Parker, 2019; Lopez-Hilfiker et al., 2019; Zeng et al., 2020; Brown et al., 2021), whose actual species may have elemental composition of $C_{16/18}H_{30-34}O_{3-6}$. Particle-phase reactions between possible peroxides (such as $C_7H_{12}O_5$ and $C_9H_{16}O_5$ that abundant in V-OxiGen^{1st}-Gly and LV-OxiGen^{1st}-Gly^{TD}) and substituted alcohols or aldehydes ($C_6H_{12}O_3$ or $C_6H_{10}O_3$, etc.) accelerated in thermal desorption at lower oxidative stage may also be an alternative source(Luo et al., 2024; Qian et al., 2026).

4. Section 3.3 and Supplement Section S4: PMF robustness

The additional PMF evaluation is useful, but Section S4 primarily compares goodness-of-fit and residual metrics among the full, normalized, and particle-phase-only datasets. These metrics do not establish whether the same chemically meaningful factors are recovered from the different input matrices.

Please directly compare the particle-only factors with the particle-dominated SV/LV factors from the combined gas-particle analysis. This could include factor-profile similarity, time-series correlations, thermogram characteristics, dominant ions, and oxidation-stage assignments. A concise factor-matching table would be helpful. The authors should identify which factors and conclusions are reproduced across the alternative analyses and discuss factors that are sensitive to the selected dataset. A gas-phase-only sensitivity analysis would also be useful, or its omission should be explained.

Response: Thank you for your advice. To further confirm the applicability, we calculate the contrast angle between factors in ME-2 PMF results utilizing full time-series, particle-phase only, and normalized time-series data as input. The results show fine similarity between

corresponding factors in full-time series methods and normalized time series method both with best factor number show in Table S4.1, which indicate that full-time series method is able to extract the variation of species. Moreover, similarity between particle-phase only factors and full time series factors are even closer, indicating the ability for full-time series methods to extract particle-phase characteristics. In conclusion, we would choose full-time series as the basic ME-2PMF data processes.

In conclusion, we would prefer choosing ME-2 PMF as factorization algorithm, select full time series data as main data pre-treat method for PMF in this article, while treat results of particle-phase only data to volatility and partitioning results as reference. To strengthen the confidence in utilizing full time series data as input of ME-2 PMF, we compared composition characteristics of results from different data selection methods with best factor number shown in Table S4.1. We estimate the similarity between data from each pre-treat methods by calculating contrast angle between intensity distributions of factors decomposed from input data. The results are shown in Figures S4.13-S4.14. Figure S4.13 shows that composition characteristic extracted from normalized time series has similar characteristics to full time-series data, with contrast angle of nearest factors between these two methods are 30~40°. Figure S4.14 indicate that factors extracted from particle phase only data are corresponding to factors extracted from full time-series data, where contrast angle of nearest factors between these two methods are less than 10°. Comparison result indicate the best applicability of utilizing full time-series data as ME-2 input, thus strengthen our confidence on full time-series methods.

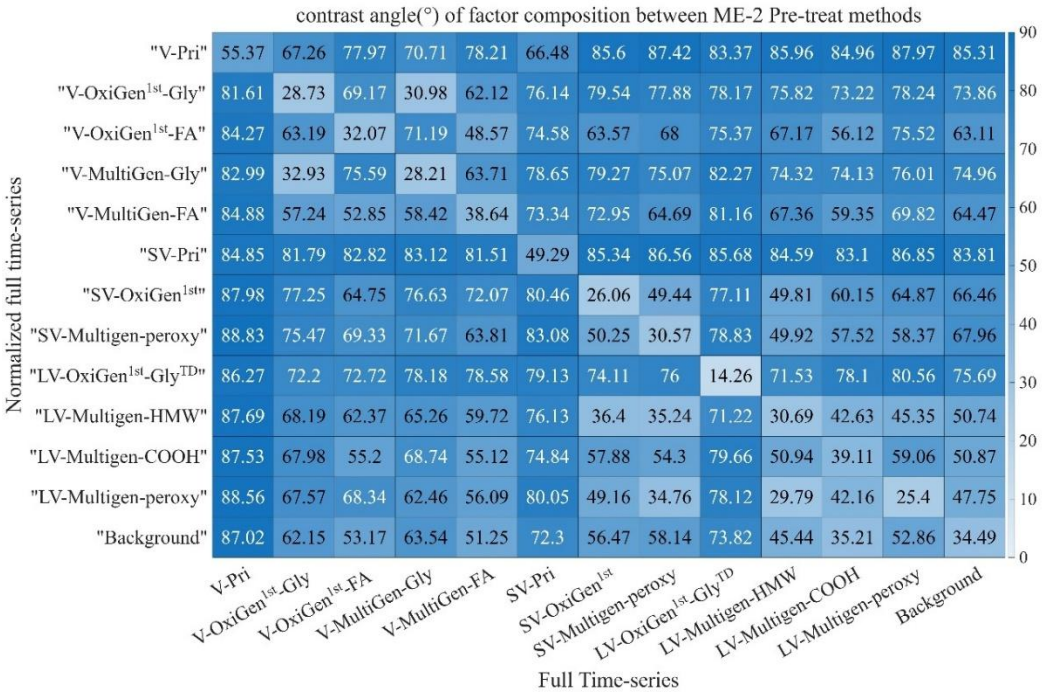

Figure S4.13 in SI. Contrast angle in degree between factors resolved by ME-2 PMF utilizing full time series and normalized time series as database selection method

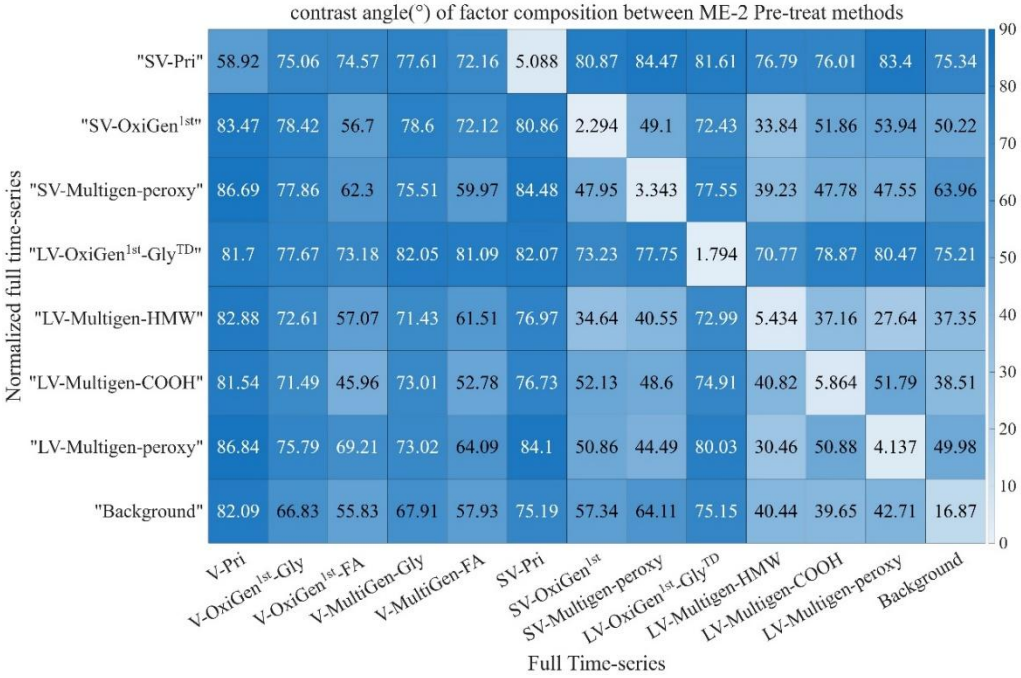

Figure S4.14 in SI. Contrast angle in degree between factors resolved by ME-2 PMF utilizing full time series and particle phase only time series as database selection method

Table S1.1 in SI Possible best factor number list of factorization algorithms with various data pre-treat methods. Red bold number shows the chosen best factor number among results in certain factorization and pre-treat method

Possible best factor number	Full time series	Normalized full time series	Particle-phase only
ME-2 PMF	6,10,11,**13**,15	8,11,**13**,15	**8**,9,12,14
MATLAB® NNMF	6,**10**,15	7,**11**,15	**6**,9,12

5. Line 230

Please correct "pervious researches" to "previous studies."

Response: Thank you for your advice. We have examined and corrected the typos in this article.

6. Line 240

Please refer directly to the Supplement section and figure where the Background factor and the criteria used to classify it as contamination are described, for example, Section S4 and the relevant thermogram.

Response: Thank you for your advice. The descriptions in section 3.3 are shown below:

Among factors, we would first classify the 13th factor as more closely to a background factor as shown in **Fig. S6.4** due to unreasonable thermogram including ill-shaped multiple distinct peaks at different desorption temperature. This factor is named Background, apart from other factors classified by volatility and oxidative states. Intensity of factor Background is relatively low, showing that contaminant would not be able to interfere measurement result too much.

And discussion in section S4 in SI is shown below:

The factors obtained from PMF are classified with oxidative state and volatility. First, the 13th factor named Background is considered contaminant factor because of its unreasonable Thermogram characteristic. The contamination factor consists of 3 separated peaks at totally separate desorption temperatures, implying that it may consist of three parts related to different interference. Low-desorption-temperature portion may contain interference from FIGAERO inlet model shifting that may mix gas-phase components with aerosol-phase, which can be observed at the first couple of seconds of particle phase data. Medium- and higher-desorption-temperature portions may originate from semi-volatile and low-volatile residuals.

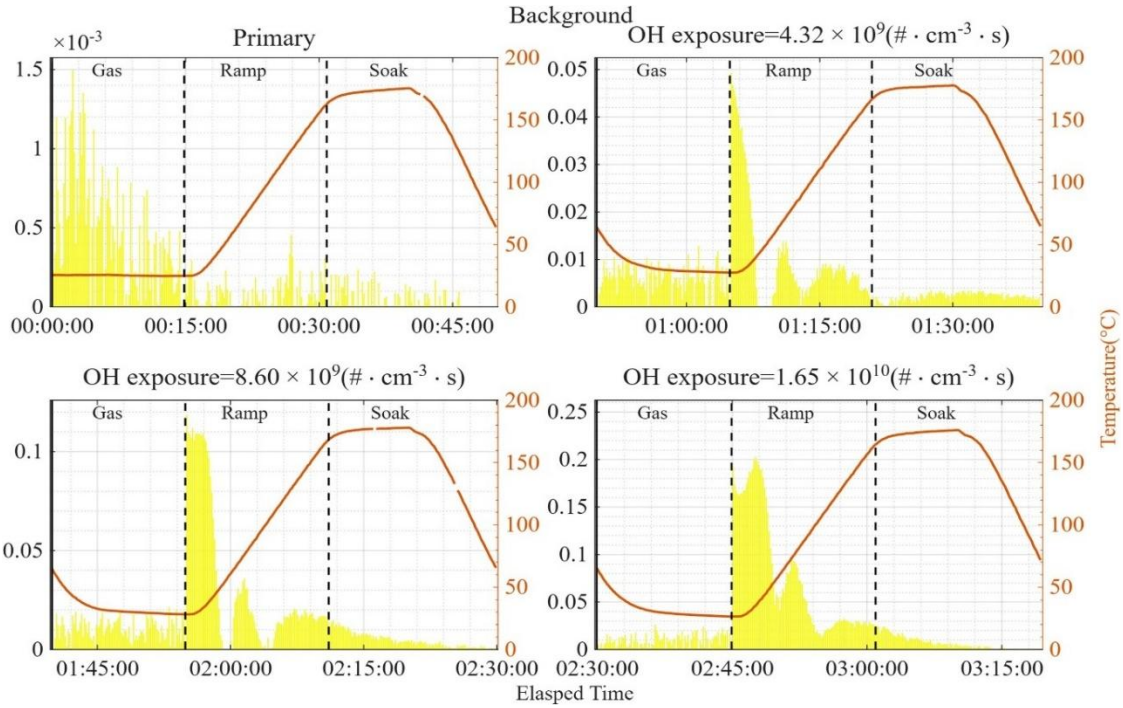

Figure S6.4 in SI Intensity time series FIGAERO measurement circles of contamination factor Background from ME-2 PMF results at different OH exposure during FIGAERO measurement circles.

7. Line 284

Please define the suffix "TD" when "LV-OxiGen1st-GlyTD" is first introduced. If it denotes thermal decomposition or a thermal-desorption-related factor, this should be stated explicitly.

Response: Thank you for your advice. The TD here means "Thermal Decomposition", which means that these compounds are originated from thermal decomposition of oxidation products that keep long-chain fatty acid structure. Modified paragraph in section S3.3 are shown below:

Factor LV-OxiGen^{1st}-Gly^{TD} have similar average oxidative state and molecular size with V-OxiGen^{1st}-Gly, seems corresponding to gas phase portion of first-generation oxidation products represented by V-OxiGen^{1st}-Gly. However, thermal desorption thermogram of LV-OxiGen^{1st}-Gly^{TD} peaks at ~440K, showing that compounds represented by LV-OxiGen^{1st}-Gly^{TD} have much lower volatility than molecular composition corresponding to this factor, indicating that LV-OxiGen^{1st}-Gly^{TD} representing thermal decomposition

fragmentations of oxidation products with long-chain fatty acid structure (Frankel et al., 1983; Patrikios et al., 1994; Martins et al., 2013; Aladedunye, 2016; Bonetti and Parker, 2019; Lopez-Hilfiker et al., 2019; Zeng et al., 2020; Brown et al., 2021), whose actual species may have elemental composition of $C_{16/18}H_{30-34}O_{3-6}$. Particle-phase reactions between possible peroxides (such as $C_7H_{12}O_5$ and $C_9H_{16}O_5$ that abundant in V-OxiGen^{1st}-Gly and LV-OxiGen^{1st}-Gly^{TD}) and substituted alcohols or aldehydes ($C_6H_{12}O_3$ or $C_6H_{10}O_3$, etc.) accelerated in thermal desorption at lower oxidative stage may also be an alternative source(Luo et al., 2024; Qian et al., 2026).

8. Lines 347-351

The sentence beginning "Varying the mass accommodation coefficient from 1 to (10^{-4})…" is repeated and one occurrence should be deleted. In addition, insensitivity to the assumed accommodation coefficient does not by itself demonstrate a liquid-like particle phase. Any phase-state inference should instead be linked to the viscosity estimates and their assumptions.

Response: Thank you for your advice. The liquid-like particle phase is based on low viscosity and particle-phase diffusion time scale estimations. As shown in section 3.4, the particle-phase diffusion time scale in primary and secondary organic aerosols are 10^{-2}~10^{0}s, corresponding to viscosity 10^{4} Pa·s(utilizing elemental composition parametrization methods developed by DeReiux,2018 and Li,2020), indicating weak-limited particle phase diffusion and near-liquid semi-solid particle phase. Utilizing other parameterizations methods (e.g. tGBoost methods, Galezzo 2022) would result in an even lower viscosity at 10^{1} Pa·s corresponding to fully liquid aerosol phase. The Modified section S3.4 part of kinetic estimations are shown below:

Gas-particle partitioning is governed by both thermodynamic and kinetic processes. We compared characteristic time scales (τ) for gas-phase diffusion, surface desorption, and particle-phase diffusion with time scales apart from gas-particle partitioning served as reference, including particle coagulation, oxidation of cooking precursors (e.g., oleic acid), and residence in the Go:PAM. Detailed kinetic and thermodynamic estimation and parameterization methods are shown in Section S5 of Supplement S1, and the results are shown in Figure 4. Note that the kinetic estimations are based on Fickian diffusion and the fractional Stokes-Einstein relationship, which can undergo violation in secondary organic aerosol, especially for small molecules in in highly-oxidized aerosol(Marshall et al., 2016; Bedoya-Lora et al., 2019; Evoy et al., 2021; Mutneja and Karmakar, 2025). To ensure whether Fickian diffusion and fractional Stokes-Einstein relationship is adaptable in this system, Deborah number and Maxwell-Stefan diffusion coefficients are calculated and utilized to evaluated their applicability, as described in Section S5 of Supplement S1. (Preston and Zuend, 2022). Results are shown in Figures S6.42-6.44 of Supplement S1, indicating that deviations from the fractional Stokes-Einstein relationship and Fick's law are not expected to control the kinetics of the primary or secondary cooking aerosol under the investigated conditions, thus clarify the applicability of kinetic estimation utilized in this study(Pastore et al., 2021; Evoy et al., 2021; Preston, 2022).

Among gas-particle partitioning processes, particle-phase diffusion is the fastest modelled process in both primary and secondary aerosols across the investigated OH exposures, with τ values of approximately 10^{-2}–10^{0} s, substantially shorter than the 55 s residence time and

the oxidation time scale of primary precursors, implying minor resistance of particle-phase diffusion on gas-particle partitioning under the modelled conditions. The reason of rapid particle-phase diffusion is liquid-like phase-state nature of primary and secondary organic aerosols regardless of viscosity parameterization methods, shown in Figure S6.45-46. Gas-phase diffusion time scale varied with both OH exposure and molecular weight. In primary aerosol, for most species with molar weight <150 g mol^{-1}, gas-phase diffusion time scale is over 104 s, significantly slower(>3 order of magnitude) than any other processes in gas-particle partitioning and reference time scale, leading to more gas-phase-abundant partitioning compared to equilibrium state; for species with molar weight>150 g mol^{-1}, gas-phase diffusion time scale are comparable with coagulation time scale while still longer than other processes (about 1 order of magnitude). In the secondary aerosol, for some low-molecular-weight compounds with molar weight <120 g mol^{-1}, gas-phase diffusion time scale is still longer than retention time and oxidation time scale (about 1 order of magnitude); for other components, gas-phase diffusion time scale is shorter than retention time and oxidation time scale, with similar value to coagulation time scale (less than 1 order of magnitude). Surface-desorption time scales increase drastically with molecular weight: species with molecular weight >200 g mol^{-1} have desorption times longer than the residence time and account for approximately 10% of the total detected mass, whereas species with molecular weight >300 g mol^{-1} have desorption times longer than 1 h and account for approximately 5%. Surface desorption may therefore retain a limited fraction of high-molecular-weight compounds. In primary aerosols, large molecules with molar weight >250 g mol^{-1} would have both gas-phase diffusion and surface desorption time scale significantly longer than retention time, resulting in stable gas-particle partitioning characteristic only related to initial emission regardless of kinetic and thermodynamic property change. In secondary aerosols, $C_{>9}O_{>5}$ peroxides and auto oxidation products keeping long-chain fatty acid structures ($C_{16,18}O_{>4}$) would be confined to remain at aerosol phase due to kinetic limits in surface desorption process. Meanwhile, influence of surface desorption on semi- and intermediate- volatile components remains minor. Faster particle-phase diffusion and slightly slower gas-phase diffusion than coagulation is consistent with conclusions shown in Section 3.1, that the dominate SOA growth driving force is both condensation and coagulation. It should be noticed that, adsorption onto surface have already been considered in gas-phase time scale of gas-phase diffusion processes, utilizing the effective mass accommodation coefficient α_{eff} recommended by Shiraiwa et al.(Shiraiwa and Pöschl, 2021) accounting for particle-phase near-surface mass transport, rather than the pure surface accommodation coefficient α_s. Varying the surface mass accommodation coefficient from 1 to 0.01 by utilizing different α_s estimation methods would lead to significant variation of gas-phase diffusion time scale, while have minor effect on aerosol-phase diffusion time scale (Figure 4 and Figures S6.48-6.49), while ignoring near-surface mass transfer would have similar or higher changes to gas-phase mass transfer time scale (Figures S6.50). This finding strengthens the suggestion on liquid-like, little-kinetic-limit aerosol phase of secondary cooking aerosol, indicate importance of surface processes (including surface accommodation and desorption) in gas-particle partitioning (Lbadaoui-Darvas et al., 2021; Knopf et al., 2024). We concluded a molecular-weight-dependent kinetic influence on gas-particle partitioning. Partitioning in

primary aerosols consist of gas-phase favored partitioning for species with molar mass<250 g mol^{-1} and emission-determined partitioning for species with molar mass>250 g mol^{-1}. Partitioning in primary aerosols consist of gas-phase favored partitioning for small molecules with molar mass<120 g mol^{-1}, near-equilibrium partitioning for major components with molar mass between 120 g mol^{-1} and 220 g mol^{-1}, and particle-phase favored partitioning for large molecules with molar mass>220 g mol^{-1}. Results show consistency with the minor changes on bulk composition because of possible major contribution of condensation onto particles rather than continuous oxidation the reason is that rate-determining step is gas-phase diffusion. Results are comparable to previous studies on primary and secondary cooking aerosol under the studied OH-exposure range (<10^{10} molecules cm^{-3} s)(Takhar et al., 2021; Masoud et al., 2022; Hou et al., 2025; Liu et al., 2025).

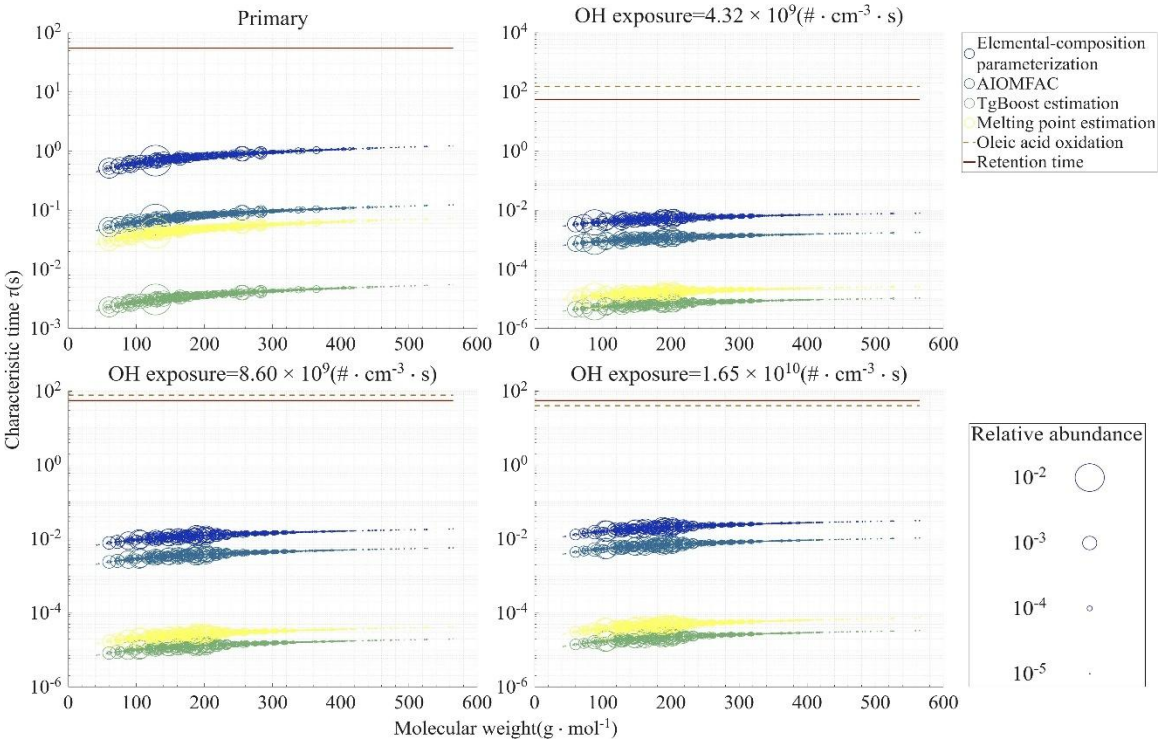

Figure S6.45 In SI Influence of various viscosity estimation method on particle-phase diffusion time scale of primary and secondary organic aerosols. Blue: 2-D-VBS based parametrization; blue-green: AIOMFAC-VISC; green: tgBoost method; yellow: melting point method.

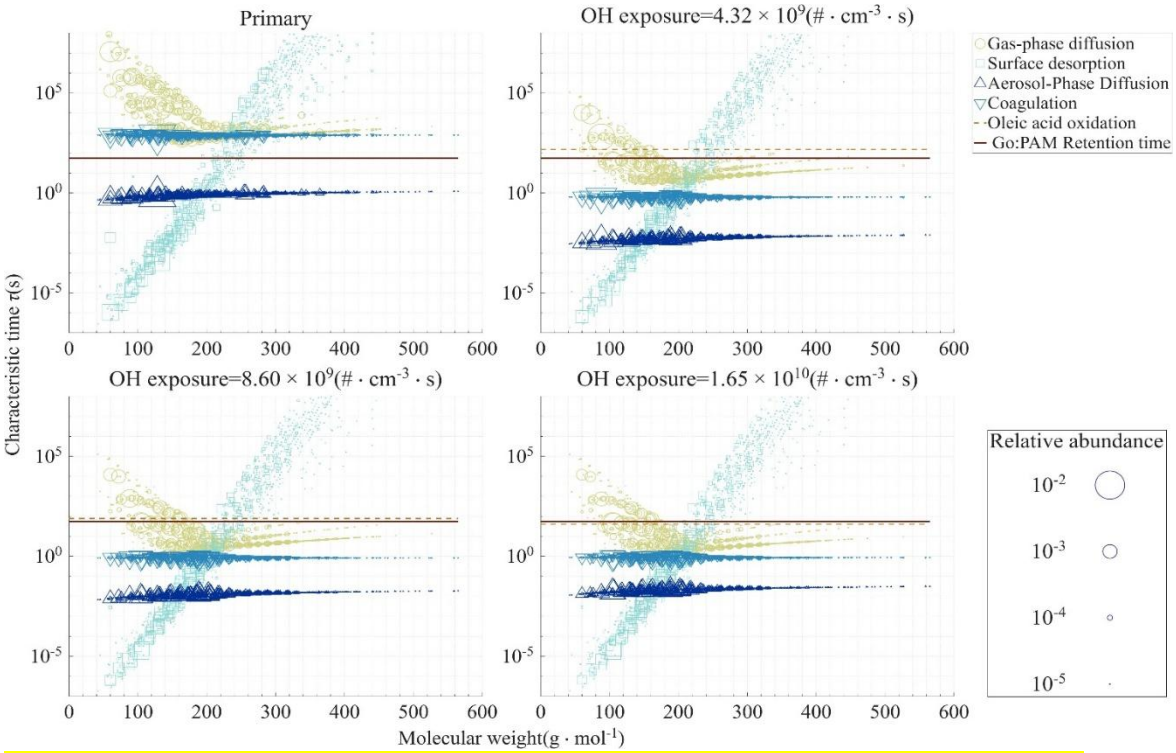

Figure 3 in Main Text The characteristic time scale of FIGAERO-CIMS detected species in various kinetic transport processes of gas-particle partitioning with enhancement of OH exposure. Markers show time scale of gas-phase diffusion(circle), surface desorption(square), aerosol-phase diffusion(triangle), coagulation (reverse triangle). Lines shows reference time scale, including retention time(solid) and oleic acid oxidation(dashed). Marker size represents relative abundance of species. Surface mass accommodation coefficients are estimated based on parametrization method 1 shown in Section S5.

9. Conclusion

The conclusion currently reads mainly as a summary. Please provide more specific implications of the PMF and partitioning results—for example, whether the proposed factors or molecular markers could help identify cooking-derived primary and secondary material in ambient measurements, and how the inferred near-equilibrium behavior of most secondary S/IVOCs could inform atmospheric models. These implications should remain within the scope of the experiment. Because only heated corn oil was studied under controlled laboratory conditions, the results cannot determine which cooking activities or food types have the greatest SOA-forming potential. This limitation should be stated clearly. Finally, the manuscript would benefit from careful language editing, as numerous grammatical and sentence-structure problems remain.

Response: Thank you for your advice. We have added conclusions and implications into section 4 of the revised manuscript. The results in this article can therefore be extent to any other sources and oxidation products, where precursors having long-chain hydrocarbon-like structure, and OH radical as oxidant. These components include the reason is similar oxidation mechanism and compound distribution. The modified Section 4 are shown below:

This study presents a comprehensive investigation into the atmospheric evolution of cooking-derived organic aerosols, integrating advanced analytical techniques to unravel

complex gas-particle dynamics. Using a Go:PAM oxidation flow reactor together with FIGAERO-I-CIMS measurements, we characterized changes in molecular composition, volatility, and gas-particle partitioning across the investigated OH exposures. A key innovation lies in the combined application of high-resolution mass spectrometry with a two-dimensional volatility basis set (2-D VBS) framework, enabling a mechanistic understanding of composition-dependent partitioning behavior.

Under typical atmospheric conditions, primary cooking emissions rapidly generated substantial quantities of fine particles (~10 nm) within two hours, followed by the formation of higher concentrations of 30–50 nm secondary aerosols over 0.5-1 days. Notably, oxidation products predominantly occupied the semi-volatile and intermediate-volatility organic compounds (S/IVOCs) range in the 2-D VBS, systematically migrating toward the SVOC region as oxidation progressed, while molecular weight and oxidation degree remained relatively stable. Leveraging positive matrix factorization (PMF), we systematically classified compounds by oxidation degree and volatility, identifying representative markers across evolution stages: gaseous glycerol and particulate long-chain fatty acids in primary emissions; medium-weight carbonyl acids (e.g., $C_5H_{10}O_3$, $C_7H_{12}O_3$) as intermediate products, and multi-generation oxidation products including dicarboxylic acids (e.g., $C_9H_{16}O_4$) and HOM-like compounds (e.g., $C_{18}H_{32}O_{5-6}$) as mature products. Of particular importance are highly oxidized small organic acids ($\leqslant C_3$) and multi-generation products in the C_7-C_{10} range with moderate volatility and high oxidation state.

A central finding concerns the thermodynamics and kinetics gas-particle partitioning observed across different compound classes. Observation shows that fragmentation-derived functionalized multi-generation oxidation products exhibits near equilibrium state, and identified significant kinetic limitations for first-generation oxidation products ($C_{3-8}O_{3-4}$) and large non-cleavage products ($>C_{14}O_5$), which exhibited significant deviations from equilibrium. Based on comprehensive estimation and parametrization of kinetic and thermodynamic processes, we concluded that the secondary cooking aerosol in this study are near equilibrium state for typical secondary S/IVOCs that are predominant in this study, while partitioning in primary aerosols, and for low-molecular-weight and high-molecular-weight species in secondary are constrained Surface processes account for most gas-particle partitioning kinetic limits for most non-equilibrium-partitioning compounds . Thermodynamic analysis unravels gap between theory and measurements especially for small and large molecules, requiring further instrumentation and theory development. The mechanistic insight into partitioning dynamics represents a significant advance in understanding the atmospheric behavior of cooking emissions, given clear evidence in a liquid-like and weak kinetic limited aerosol phase and a surface-mass-transfer limited gas-particle partitioning scheme for cooking and even other anthropogenic and natural emissions with OH radical as oxidant and long-chain-hydrocarbon-like species as precursors. Our results provide a scientific foundation for refining emission inventories and air quality models, ultimately contributing to improved exposure assessment and mitigation strategies for urban and indoor environments.